Biochemistry

 Volume 41, Number 13 April 2, 2002

Current Topics

The Alternating Site, Binding Change Mechanism for Proton Translocation by Transhydrogenase†

J. Baz Jackson,* Scott A. White, Philip G. Quirk, and Jamie D. Venning

School of Biochemistry, University of Birmingham, Edgbaston, Birmingham B15 2TT, U.K.

Received November 21, 2001; Revised Manuscript Received January 10, 2002

Transhydrogenase is located in the inner membrane of animal mitochondria and in the cytoplasmic membrane of many bacteria. It couples the redox reaction between NAD(H) and NADP(H) to the translocation of protons across the respective membrane:

$$NADH + NADP^+ + nH^+_{out} \leftrightarrow NAD^+ + NADPH + nH^+_{in} \quad (1)$$

where n is probably 1.0 (*1*). The redox reaction is stereospecific: a hydride ion equivalent is transferred from the A side of NC4 of NADH to the B side of NC4 of $NADP^+$ (*2*). The $\Delta G^{\circ\prime}$ of the reaction in solution is close to zero. Thus unusually, perhaps uniquely, for an ion translocator of this type, the free energy of the ion electrochemical gradient is conserved only in the concentration term of ΔG of the scalar chemical reaction.

Two simple observations, taken together, indicate that coupling of transhydrogenase to proton translocation does not occur at the redox step. (a) There is no intrinsic hydrogen exchange between the reduced nucleotide and water protons during enzyme turnover (*2*). (b) The transfer of hydride equivalents between nucleotides is direct; there are no redox intermediates (*3*, *4*). Coupling is achieved by linking protonation/deprotonation associated with the ion translocation reaction to changes in conformation of the protein and nucleotide. In this sense, the mechanism of transhydrogenase might have features in common with the conformationally coupled, ion-transporting ATPases, a concept that will be explored in this review.

For recent reviews of the proton-translocating (or "AB") transhydrogenase, see refs *5*−*9*. Because of space limitations, we are unable to cite all the recent work, including many mutagenesis experiments, that has been carried out on the enzyme. Our web site (http://www.biochemistry.bham.ac.uk/transhydrogenase) carries a complete list of all mutagenesis work.

Physiological Roles of Transhydrogenase. Transhydrogenase operates at an important three-way interface in metabolism: between the two, major, soluble redox cofactors of the cell and the proton electrochemical gradient (Δp), which serves as the energetic intermediate between the respiratory chain and ATP synthase. There are no known allosteric regulators of the enzyme. In many conditions in vivo, the enzyme probably operates close to equilibrium. Thus, Δp is typically in the order of 0.2 V, the NAD(H) pool is mainly oxidized, and the NADP(H) pool is highly reduced. In bacteria, the product NADPH is used in metabolic biosynthesis (*10*) and to reduce glutathione, e.g., to protect against oxidative stress (*11*). The function of the enzyme in mitochondria is broadly similar (reviewed in ref *12*) but is tissue dependent; e.g., the NADPH generated is used for steroid synthesis in adrenal and kidney cells and in protection against free radical damage in liver. In muscle mitochondria, transhydrogenase is thought to have a controlling influence on flux through the tricarboxylic acid cycle; it drives a "minicycle" between isocitrate and 2-oxoglutarate and therefore amplifies the response of NAD-linked isocitrate

† Financial support was provided by the Wellcome Trust and the Biotechnology and Biological Sciences Research Council.

* To whom correspondence should be addressed. Phone: +44 (0)-121 414 5423. Fax: +44 (0)121 414 5925. E-mail: j.b.jackson@bham.ac.uk.

10.1021/bi012078d CCC: $22.00
Published on Web 03/08/2002

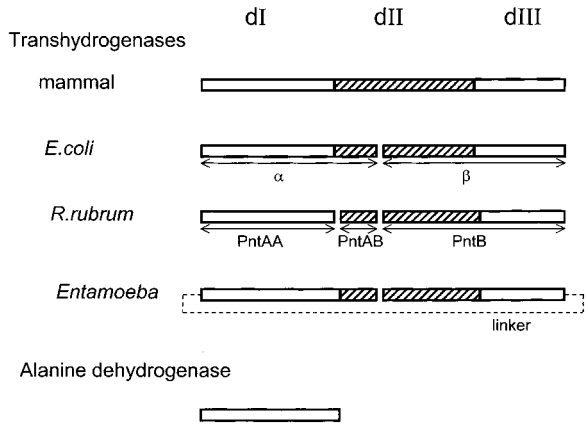

FIGURE 1: Polypeptide structure of transhydrogenases from different species. The four different types of polypeptide organization found in the transhydrogenases are shown, with one example of each type. The peripheral NAD(H)-binding component (dI) and NADP(H)-binding component (dIII) are unshaded. The membrane-spanning dII is shaded. The sequence similarity between dI and alanine dehydrogenase is also illustrated.

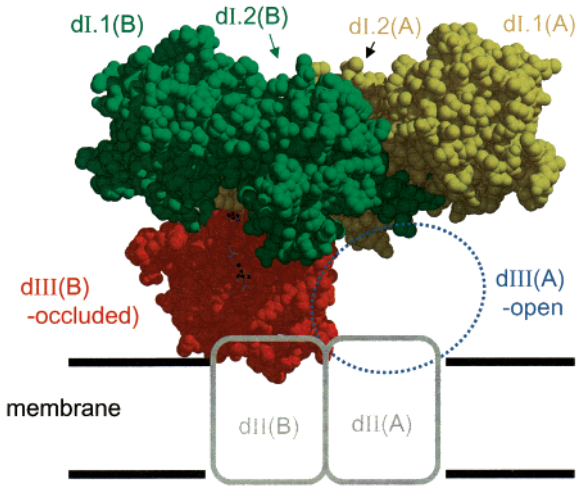

FIGURE 2: Space-filling model of the X-ray structure of the dI_2-$dIII_1$ complex and its expected relationship with the intact transhydrogenase. The color coding of the dI_2dIII_1 complex is similar to that in later figures. The description of dIII as either occluded or open is explained in The Reciprocating, Alternating Sites of Transhydrogenase.

dehydrogenase to its allosteric regulators (*13*). Transhydrogenase can operate in reverse (cf. eq 1). For example, in anaerobic cestode parasites, using NADPH produced by the action of the malic enzyme, transhydrogenase operates as a generator, rather than a consumer, of Δp (*14*). In the protozoan parasite, *Entamoeba histolytica* transhydrogenase is located in mitochondrially derived organelles called mitosomes which lack the enzymes of oxidative phosphorylation (see ref *15*); here the partner of transhydrogenase in its chemiosmotic proton circuit is unknown. Transhydrogenase does not appear in the genome of the plant *Arabidopsis thaliana*. The distribution of transhydrogenases in other species is listed on our web site.

Subunit Composition of Intact Transhydrogenase. Transhydrogenases from mitochondria and from bacteria appear to have quite similar molecular sizes and structures, although there are differences in polypeptide organization (Figures 1 and 2). Transhydrogenase from the mitochondria of multicellular animals is a homodimer of two polypeptide chains, each with ~1000 amino acid residues (*16*). In bacteria there are two variations on this theme. The enzyme from *Escherichia coli* and some other species has an amino acid sequence similar to that of the transhydrogenase of higher animals but is split into PntA and PntB polypeptides (α and β) having ~510 and ~460 amino acid residues, respectively (*17*). At least in *E. coli*, these are organized in an $\alpha_2\beta_2$ unit. In *Rhodospirillum rubrum* and some other species, PntA is further split into PntAA (~380 residues) and PntAB (~140 residues); PntB (~460 residues) remains similar to that of the *E. coli* transhydrogenase (*18*, *19*). The X-ray structure of subcomplexes of the *R. rubrum* enzyme (*20*) again suggests an overall "dimeric" structure: $(PntAA)_2(PntAB)_2$-$(PntB)_2$. The enzymes in some protozoan parasites have evolved along slightly different lines. Their transhydrogenases comprise a single polypeptide whose N-terminus corresponds to that of bacterial PntB. The C-terminus of the PntB-like sequence is linked (through an extra ~40 amino acid residues) to the equivalent of the N-terminus of PntA. An overall dimeric organization is again likely (C. J. Weston and J. B. Jackson, unpublished).

Despite these variations in polypeptide organization, all proton-translocating transhydrogenases have three major structural components, designated dI,[1] dII, and dIII, which probably assemble with a universal topology. The positions of these components are mapped onto the polypeptides of representative species in Figure 1. Both dI, which binds NAD^+ and NADH, and dIII, which binds $NADP^+$ and NADPH, protrude from the membrane, on the matrix side in mitochondria and on the cytosolic side in bacteria. The dII component spans the membrane. In all bacteria and in the protozoan parasites, dII is split into dIIa and dIIb, but this is not expected to affect the overall topology. Transhydrogenase has been depicted with substantial contact surfaces between each of the three major components, but recent data suggest that such an organization is unlikely (*20*). Instead, as illustrated in Figure 2, dI is largely separated by dIII from the membrane-spanning dII. When dI and dII are on the same polypeptide, the linking region (whose sequence is not well conserved) must be structurally rather extended and is presumably mechanistically unimportant.

Because of the different arrangements, it is helpful to refer to the complete, intact transhydrogenase as a generic dimer of dI:dII:dIII "trimers", while recognizing that in mammals this corresponds, in polypeptide terms, to a $(dI\text{-}dII\text{-}dIII)_2$ dimer, in *E. coli*, to a $(dI\text{-}dIIa)_2(dIIb\text{-}dIII)_2$ tetramer, in *R. rubrum*, to a $(dI)_2(dIIa)_2(dIIb\text{-}dIII)_2$ hexamer, and, in protozoan parasites, to a $(dIIb\text{-}dIII\text{-}dI\text{-}dIIa)_2$ dimer.

Biochemical Resolution and Reconstitution of the Membrane Peripheral Components of Transhydrogenase. Using recombinant DNA techniques, the dI and dIII components of transhydrogenases from several species have been isolated as stable, water-soluble proteins and purified (*21*−*28*). In some species (e.g., *R. rubrum*), the dI component of transhydrogenase naturally exists as a separate polypeptide (PntAA); see Figure 1. In others, the introduction of a stop codon into *pntA* is required for the production of isolated

[1] Abbreviations: dI, the NAD(H)-binding component of transhydrogenase; dII, the membrane-spanning component; dIII, the NADP(H)-binding component; $AcPdAD^+$, acetylpyridine adenine dinucleotide (oxidized form).

dI. The dIII component never corresponds to a separate polypeptide, and its isolation always requires genetic engineering.

A simple mixture of the dI and dIII components forms a complex (Figure 2) which can catalyze transhydrogenation between NAD(H) and NADP(H) or their analogues. The character of this complex and a comparison of the nucleotide-binding properties of isolated dI and dIII with those of the complex and of the intact enzyme provide insights into the mechanism of hydride transfer and proton translocation. The following fundamental observations serve as a basis for further discussion:

(a) In solution, isolated dI components are dimeric (*21*, *29*−*31*). The *R. rubrum* dI protein is also dimeric in the crystalline state (*20*, *32*). The protein binds NAD^+ and NADH with rates and affinities that are comparable with the properties of the intact transhydrogenase, though there are some intricacies (*21*, *31*, *33*−*35*).

(b) In solution, isolated dIII is monomeric (*23*, *25*, *27*, *31*, *36*). At neutral pH, the protein binds $NADP^+$ and NADPH extremely tightly (*23*, *25*, *27*), with a much higher affinity than that of the intact enzyme ($>10^4$ fold).

(c) The complex formed from isolated dI and dIII from *R. rubrum* transhydrogenase, in solution (*31*) and in the crystalline state (*20*), is a stable dI_2dIII_1 heterotrimer. Dissociation of the trimer into dI_2 and dIII has a $K_d \approx 25$ nM. NMR experiments show that the dI_2dIII_2 tetramer can form at high protein concentrations (*36*): its dissociation constant exceeds 100 μM (*31*).

The tight binding of NADP(H) to isolated dIII and the asymmetry revealed in the dI_2dIII_1 heterotrimer might be significant in the elucidation of the mechanism of proton translocation.

High-Resolution Structure of the dI_2dIII_1 Heterotrimeric Complex of Transhydrogenase. The crystal structure of the dI_2dIII_1 complex of the *R. rubrum* transhydrogenase was recently solved to a resolution of 2.5 Å [PDB 1HZZ (*20*)]. It follows earlier determinations of structures of the isolated *R. rubrum* dI component [IF8G (*32*)], isolated bovine dIII [1D4O (*37*)], human dIII [1DJL (*8*, *38*)], and a solution (NMR) structure of *R. rubrum* dIII [1E3T (*39*)]. A solution structure of the *E. coli* dIII is also in progress (*40*, *41*).

(1) The NAD(H)-Binding Component (dI). The two dI polypeptides (A and B) in the *R. rubrum* dI_2dIII_1 complex have similar though not identical conformations. Both comprise two domains (dI.1 and dI.2), each of which has the form and connectivity of a Rossmann fold (*42*): a twisted sheet of parallel β-strands flanked by helices. The two $\beta\alpha\beta\alpha\beta$ motifs and the "crossover helix" of the classical Rossmann structure are easily recognized in each domain. In polypeptide A, a molecule of NAD^+ is associated mainly with the dI.2 domain: the binding crevice for the adenosine moiety, at the C-terminal edge of the β-sheet, is fundamentally similar to that found in many other Rossmann structures. There is a G-X-G-X-X-G "fingerprint". Specificity for NAD(H) relative to NADP(H) is determined at least partly by the interaction between the carboxylate of invariant D202 and the 2′- and 3′-OH groups of the adenosine ribose. There must be another NAD^+-binding site in the equivalent position of polypeptide B, though the electron density is weak and a nucleotide molecule was not fitted in the model (see below). The two domains of each polypeptide of dI are linked by the relatively long helices, α6 and α11, and they are separated by a deep cleft (Figure 3), in which resides the nicotinamide mononucleotide moiety of the bound NAD^+ (at least in polypeptide A). The dI polypeptides are positioned around a 2-fold axis of pseudosymmetry in such a way that the two clefts point away from each other in the dimer. There are extensive contacts in the dimer interface: the two dI.2 domains form a central core, whereas the two dI.1 domains are more peripheral.

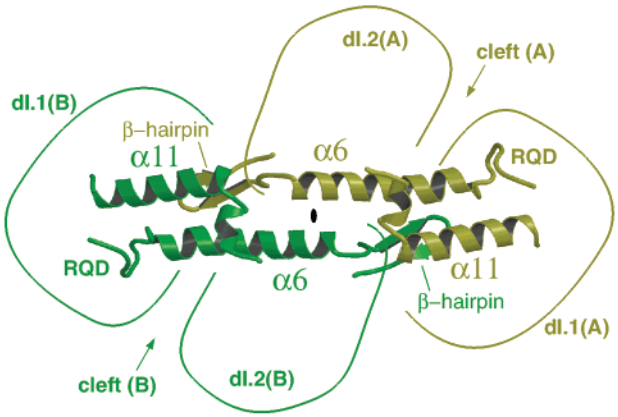

FIGURE 3: Symmetrical organization of helices α6 and α11 across the dI dimer (viewed from the top of Figure 2). The oval spot shows the 2-fold axis of pseudosymmetry.

The amino acid sequence and the three-dimensional structure of dI are similar to those of the soluble protein, alanine dehydrogenase (Figure 1). Perhaps the common ancestor of these two proteins was recruited by a membrane protein (the equivalent of dII/dIII) during the evolution of transhydrogenase.

(2) The NADP(H)-Binding Component (dIII). The crystal structures of dIII reveal that it too has the form and connectivity of a Rossmann fold (*8*, *20*, *37*, *38*). The bound $NADP^+$ is located at the C-terminal edge of the β-sheet, but its orientation is reversed relative to that found in the classical Rossmann structure (*42*): the nicotinamide moiety is associated with the first $\beta\alpha\beta\alpha\beta$ motif and the adenosine moiety mainly with the second. This organization is particularly striking since the C-terminus of the first β-strand nevertheless carries a conserved, fingerprint G-X-G-X-X-V sequence, similar to that in the pyrophosphate-binding region in other dinucleotide-binding proteins. In dIII, this loop does contribute to the binding of the pyrophosphate, but it is forced into a structure different from that found in the classical Rossmann fold. The first glycine residue in the so-called fingerprint is in an uncharacteristic extended conformation, and thus the second residue (invariant Y55*)[2] protrudes from the end of the strand, where its side chain might have a role in the hydride-transfer reaction. The specificity of the dIII protein for NADP(H) relative to NAD(H) is determined by extensive H-bond interactions between the 2′-phosphate group of the former and K164*-R165*-S166* in the so-called loop E "lid". As a consequence of the reversed nucleotide

[2] Numbering of amino acid residues is for *Rhodospirillum rubrum* transhydrogenase unless otherwise stated. Amino acid numbers for isolated dIII of *R. rubrum* transhydrogenase are all designated with * (for example, Met1* of dIII = Met262 of PntB). An amino acid residue is described as invariant if it is the same in all of the 14 published species.

orientation in the Rossmann fold, the nicotinamide ring of the $NADP^+$, in its binding loop ($\beta 2-\alpha B$), is exposed at the end of a "ridge" formed by helix αB. In the dI_2dIII_1 complex, the $\beta 2-\alpha B$ binding loop and helix αB from dIII are inserted into the cleft of only the "B" polypeptide of the dI dimer. In this configuration, the dIII polypeptide has contacts with dI.2-(B), dI.2(A), and dI.1(B) but not with dI.1(A).

Transhydrogenase dIII has a fold similar to that of the FAD-binding domain of the soluble enzyme, pyruvate oxidase, and with the equivalent, but non-FAD-binding, domains of other proteins in the pyruvate oxidase family (*38*). Sequence similarities between dIII and pyruvate oxidase are barely discernible (the latter does not even have the glycine-rich fingerprint), but the NAD^+ and FAD are bound to the respective proteins in a similar way.

(3) Visualizing the Hydride-Transfer Step between Nucleotides Bound to dI and dIII in the dI_2dIII_1 Complex. Stopped-flow experiments show that the transfer of hydride ion equivalents between nucleotides bound to dI and dIII within the dI_2dIII_1 complex is direct, very fast, and has a modest deuterium isotope effect (*3*, *4*, *34*, *35*, *43*). The NC4 atoms of the two nicotinamide rings must approach one another within a few angstroms during the redox reaction. In the crystal structure of the dI_2dIII_1 complex, there is good electron density for $NADP^+$ in dIII and for NAD^+ in the A polypeptide but not in the B polypeptide of dI (*20*). The weak density in the NAD^+ binding site of dI(B), indicating either disorder or low occupancy, could result either from a conformational change due to the fact that dIII is bound at this site or from unfavorable interactions resulting from the proximity of the nicotinamide ring of the $NADP^+$ bound to dIII. This might echo the results of solution experiments which show that binding of NADH to one polypeptide of dI_2 is weaker when the dI_2 is associated with dIII·NADPH (*31*). To investigate the events accompanying hydride transfer, the NAD^+ conformation seen in dI(A) is modeled into the binding site of dI(B); see Figure 4. In this configuration, the nicotinamide rings of NAD^+ and $NADP^+$ are in the same vicinity, but the NC4 atoms are too far apart (6.5 Å) for redox chemistry. Clearly, to account for the fast hydride-transfer reaction in the dI_2dIII_1 complex, there must be movement of the protein and/or the nucleotide during turnover to bring the two atoms together.

The crystal structure of the isolated dI component provides an indication as to how this might be achieved (*32*). The asymmetric unit of this crystal has four polypeptide chains, i.e., there are two copies of the dimer, and each chain adopts a slightly different conformation. The electron densities of the nicotinamide rings of the bound NAD^+ are very weak in two of the chains and well-defined in the other two. In one of the well-defined nucleotides, the ring adopts a syn conformation relative to its ribose and is tucked into the side of the cleft. In the other, bond rotations in the NMN moiety have led to the generation of an anti conformer and to the movement of the nicotinamide ring toward the rim of the cleft. When similar bond rotations are applied to the NAD^+ modeled into the B polypeptide of the dI_2dIII_1 complex, i.e., to extend the nicotinamide ring further toward the rim of the cleft, the NC4 atoms of the NAD(H) and NADP(H) can be brought into apposition (Figure 4). No changes in the $NADP^+$ conformation are required to achieve this movement. In fact, the structure indicates that, during bond rotations of the NMN moiety of NAD^+, the binding loop of the $NADP^+$ nicotinamide, constrained by interactions with elements from dI.2(B) and dI.2(A), will serve as a fairly rigid stop. In the resulting configuration, the *pro-R* face of the NAD(H) nicotinamide would be presented to the *pro-S* face of the NADP(H) nicotinamide such that hydride transfer would take place with the known A−B stereochemistry (*2*, *44*). The reaction would occur while the NAD(H) nicotinamide is in the anti conformation and the NADP(H) nicotinamide is in the syn conformation, consistent with a commonly observed relationship in the soluble dehydrogenases (*45*). The conformational differences, seen in the structure of the isolated dI and used to reposition the NAD nicotinamide during the modeling of hydride transfer, might reflect real intermediates in the catalytic mechanism. The nucleotide conformational changes seem to be related to changes in protein conformation, especially in the polypeptide loops which originate from dI.1 and dI.2 and extend either across the cleft or alongside the nucleotide (see below).

(4) Detail at the Hydride-Transfer Site. Figure 4 shows the loops and amino acid residues that form the hydride-transfer site. The two main elements from dI are the "RQD loop" (residues 126−136) and the "mobile loop" (residues 221−240), both of which appear to be involved in the positioning of the nicotinamide ring of NAD(H) for hydride transfer. The RQD loop is at the N-terminus of the long helix, α6, which links dI.1 with dI.2, and it includes a possible "hinge" for the rigid-body relative movement of the two domains seen in the different dI conformations (*32*); see Figure 3. Amino acid side chains from the RQD loop form the dI.1 inside surface of the part of the cleft that houses the NAD^+ nicotinamide. The mobile loop protrudes from dI.2 on the opposing side of the cleft, at one edge of the β-sheet. Amino acid residues at the apex of the mobile loop approach those in the RQD loop, leading to partial enclosure of the bound NAD^+. The feature was studied by NMR before emergence of the X-ray structures (*29*, *46*−*48*). Because of its segmental mobility in the absence of nucleotides, resonances in the loop remain relatively unbroadened and are therefore easily detected. Following the binding of either NAD^+ or NADH, the loop closes down on the protein surface and makes contacts with the nucleotide. In some of the subunits seen in the X-ray structures [for example, in dI(B) of the dI_2dI_1 complex], the electron density corresponding to parts of the loop is weak, indicating disorder in the crystal and reflecting the mobility of this region in the solution state.

The important amino acid residues in these two structural elements appear to be R127, Q132, and D135 (and S138) in (and adjacent to) the RQD loop and G234, Y235, and A236 near the apex of the mobile loop. All are invariant. Different arrangements of H-bond and van der Waals interactions between these residues and the nicotinamide, the nicotinamide ribose, and the pyrophosphate groups of the NAD^+ are evident in the different subunits of isolated dI and dI(A) of the dI_2dIII_1 complex and are probably largely responsible for constraining the different conformations of the NMN part of the nucleotide in the cleft (see above). Changes in the amino acid−nucleotide and interresidue interactions in this region might thus participate in the conformational switching that is probably important in gating hydride transfer from proton translocation (see below). R127, depending on subunit conformation, can make van der Waals contacts with the

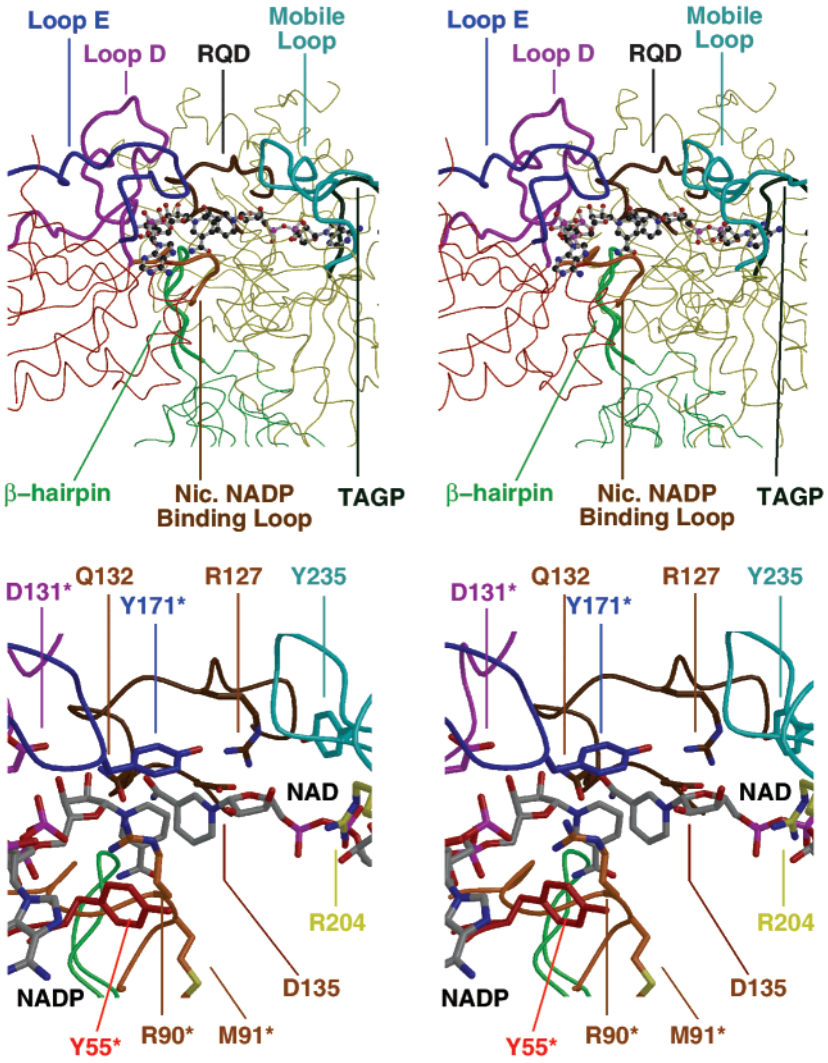

FIGURE 4: Hydride-transfer site in the dI_2dIII_1 complex (stereoviews). The upper panels show the broad perspective. The thin red line represents the dIII polypeptide chain, the thin yellow line is dI(A), and the thin green line is polypeptide dI(B). The loop regions that form the hydride-transfer site between dIII and dI(B) are shown with thick lines: dark blue, loop E from dIII; violet, helix D/loop D from dIII; light brown, the binding loop for $NADP^+$ from dIII; dark brown, the RQD loop from dI.1(B); light blue, the mobile loop from dI.2(B); black, the TAGP loop from dI.2(B); green, the β-hairpin from dI.2(A). The crystal structure of the dI_2dIII_1 complex (*20*) provides the basis for the figure, but the mobile loop region (residues 220−245) is modeled from the B polypeptide of isolated dI (*32*). The two nucleotides are shown in ball and stick format. The $NADP^+$ molecule (on the left) was derived directly from electron density in the dIII binding site of the dI_2dIII_1 complex. The NAD^+ molecule (on the right) was modeled into the dI(B) binding site using the electron density of nucleotide in dI(A) followed by rotation of the pyrophosphate and ribose bonds in the NMN moiety; see text. The lower panels show more detail. The carbon atoms of amino acid side chains are in the colors adopted for the polypeptide loops. Those of the nucleotides are in gray. The direction of the view is shifted 5° about the *x* axis relative to the upper panel.

nicotinamide ring of the bound NAD^+, and H-bond contacts with the nicotinamide pyrophosphate, with D135, S138, and Y235. Similarly, the carboxylate of D135 can be within van der Waals distance of atoms in the NAD^+ nicotinamide, and it can form H-bonds with the NAD^+ carboxamide, with R127, with L137, and with S138. Q132 is particularly interesting because, in the X-ray structure of the complex, it makes an H-bond with the 2′-OH of the nicotinamide ribose of $NADP^+$ across the dI/dIII interface, and in the modeled structure, it is within H-bonding distance of the NAD^+ carboxamide group. Thus, it might be responsible for maintaining the relative positions of the two nicotinamide rings during the hydride-transfer step. In those subunits in which electron density for the mobile loop is reasonably well-defined, Y235 can H-bond with either the NAD^+ carboxamide or with the guanidinium group of R127. This gives strong support to mutagenesis and NMR experiments from which it was suggested that the mobile loop is involved in positioning the nucleotide prior to hydride transfer (*6*). In some subunits of isolated dI and the dI_2dIII_1 complex, the mobile loop makes numerous contacts (including a salt bridge) with another loop which stretches from dI.2 across the cleft toward dI.1; in Figure 4 this is described as the TAGP loop. The A265 in this loop contacts the adenine ring of the bound NAD^+ and, of particular interest, is a van der Waals interaction between P268 and Y235. Thus a role for the TAGP loop is envisaged in the closing down of the mobile loop following the binding of nucleotide.

Another feature that helps to form the hydride-transfer site is the pair of antiparallel β-strands that extends from dI.2, which was described as the "β-hairpin". In the dI_2dIII_1 complex, the β-hairpin of the dI(A) polypeptide extends

around the back of the cleft of the dI(B) polypeptide, where it makes van der Waals contacts with the RQD loop and with the nicotinamide binding loop of $NADP^+$ in dIII. Its only invariant residues (A166-A167-G168) are located in the apical β-turn, and we suspect that its role is mainly structural (but see the Final Comments section).

There are four major secondary structure elements from dIII that contribute to the formation of the hydride-transfer site of the dI_2dIII_1 complex (Figure 4): the nicotinamide-binding loop for the $NADP^+$ (loop $\beta2-\alpha B$), loop E (the lid), the segment of polypeptide chain described as "helix D/loop D", and the segment that, in other Rossmann structures, comprises the fingerprint region at the C-terminus of strand $\beta1$. The nicotinamide-binding loop is highly conserved. It passes by the nicotinamide ring and makes extensive van der Waals contact with the *pro-R* face of the ring. Invariant R90* is especially striking; some of its C atoms are in van der Waals contact with atoms in the nicotinamide, and its guanidinium group makes an H-bond with the nucleotide pyrophosphate. Interactions with the protruding phenolic ring of invariant Y55* from the "fingerprint" region, and with that of the highly conserved Y171* from the apex of loop E, may contribute to the stability of this organization. Invariant V87* from the nicotinamide-binding loop and Y171* appear to constrain the nicotinamide ring against the binding loop. The position of loop E (it arches over the $NADP^+$ nicotinamide, its ribose, and the pyrophosphate) led to its description as the lid (*38*). It makes numerous contacts with the nucleotide and with residues in the helix D/loop D region. Together with the Y235 of the dI mobile loop, a cage-like arrangement is formed over the hydride-transfer site (Figure 4). Note that, despite the fact that most of the $NADP^+$ molecule is so deeply lodged in its dIII binding pocket, the *pro-S* (or B) side of the NC4 atom of its nicotinamide ring is fully accessible in the direction from which the nicotinamide ring of the NAD(H) can approach during the modeled rotations. It might also be significant that, following the modeled rotations, the hydroxyl group of Y171* in dIII is within H-bonding distance of atoms in the nicotinamide ribose of NAD^+ and that, like Q132 in dI (above), this could help to maintain the appropriate distance between the two NC4 atoms during hydride transfer.

Of the secondary structure elements that make up the hydride-transfer site, helix D/loop D might play a central role in the mechanism of coupling to proton translocation. It has a distinctive conformation, protruding at right angles to the β-sheet from the top of strand $\beta4$, extending for some 26 Å in an irregular helix (the N-terminus of which has multiple interactions with the pyrophosphate and ribose groups of the nucleotide), before making a series of sharp turns which take the polypeptide chain back under the helix to the N-terminus of strand $\beta5$. Conformational changes in helix D/loop D are likely to affect the adjacent RQD loop in dI and the loop E lid in dIII. A spur of amino acid residues extending through helix D/loop D and loop E experiences a distinctive magnetic change when $NADP^+$ is exchanged for NADPH (*36*). We shall return to all of these features and highlight the role of D132* in conformational changes in helix D/loop D when the energy coupling mechanism is discussed (see The Binding Change Mechanism).

Structure of the Membrane-Spanning dII of Transhydrogenase. There is no high-resolution structure of the membrane-spanning component of transhydrogenase. However, analysis of amino acid sequences and experiments on antibody reactivity and proteolytic cleavage and on labeling and cross-linking of sulfydryl groups are leading toward a consensus view as to the approximate positions of the transmembrane (TM) helices and their associated loops: mitochondrial transhydrogenases are thought to have 14 TM helices and enzymes of the *E. coli* type (Figure 1) to have 13 (reviewed in refs *49*−*51*). In *E. coli* transhydrogenase, the first 4 TM helices are associated with the α-subunit and the subsequent 9 with the β-subunit. Relative to the mitochondrial protein, it lacks the N-terminal helix of the β-subunit. Thus, the C-terminus of α is located in the cytosol, and the N-terminus of β is in the periplasm (*50*). A genetically fused transhydrogenase, with a hydrophobic linker between the α- and β-subunits, was active provided that the linker region was long enough to traverse the membrane (*52*). Those bacteria whose transhydrogenases are split into three polypeptides (Figure 1) probably have only 12 TM helices. Thus in some species from this group, the polypeptide segment corresponding to helix 1 of the mitochondrial and *E. coli* types is lacking. The missing helix (i.e., relative to the *E. coli* protein) is from PntAB, and the proposed organization requires that the N-terminus of this polypeptide is located in the periplasm. In the other species of the three-polypeptide subgroup (e.g., *R. rubrum*), the N-terminus of PntAB is not truncated. However, their TM helix 1 is only very weakly predicted, and we therefore suggest that the segment lies outside the membrane, in the periplasm. The putative TM helices in dII of *R. rubrum* transhydrogenase are shown in Figure 5. The most conserved helices (those having >3 invariant residues) are H3, H4, H9, H10, H13, and H14. Invariant residues in the TM helices are mainly disposed toward the cytoplasmic side of the membrane. Both the periplasmic and cytoplasmic loops are generally rather short. The latter (especially the loop between H12 and H13 and the C-terminal region following H4) are much more conserved.

Proton Translocation through the Membrane-Spanning dII of Transhydrogenase. A considerable number of painstaking mutagenesis experiments have been undertaken, particularly in the laboratories of P. D. Bragg and J. Rydstrom, to try to identify elements that might be responsible for proton translocation through dII. The consensus model has been that the conduction channel involves protonatable side chains of amino acid residues and bound water molecules. Well-conserved residues in the TM helices of *E. coli* transhydrogenase have been singly substituted with amino acids having nonprotonatable (or non-hydrogen-bonded) side chains (reviewed in ref *9*). All except mutants of βH91 and βN222 (equivalent to H91 and N221 in the *R. rubrum* PntB protein, Figure 5) yielded proteins with appreciable transhydrogenation activity coupled to proton translocation. The emerging conclusion is that the transmembrane region of dII is not spanned by a single, conserved conduction pathway or "proton wire". Rather, amino acid side chains and water molecules must form either a wider channel or a parallel network of proton-conducting pathway(s), perhaps converging in the region of βH91 and/or βN222. Current experiments do not eliminate the possibility that the two protomers of the dII dimer form a single proton channel.

Coupling of Proton Translocation to Transhydrogenation. Proton translocation is not intimately coupled to the redox

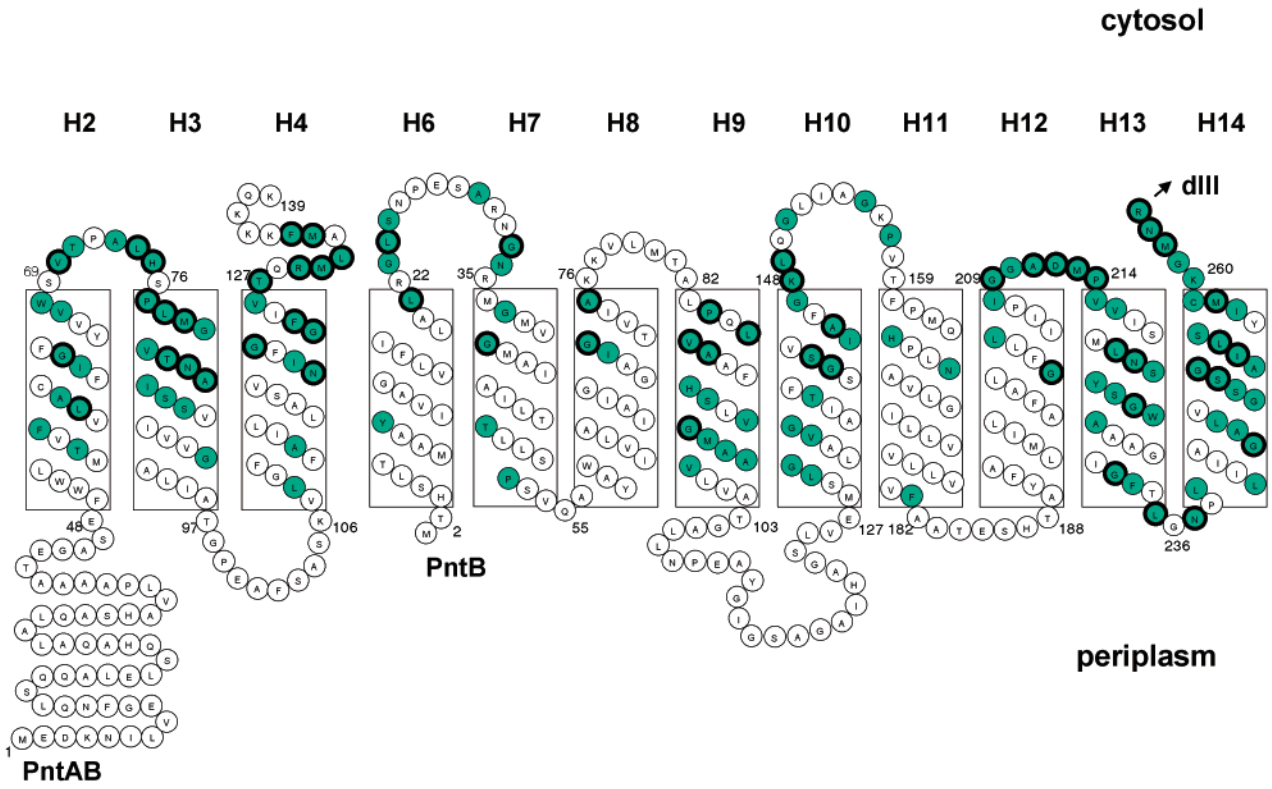

FIGURE 5: Putative transmembrane helices of *R. rubrum* transhydrogenase. TM helices were predicted using the DAS algorithm (*71*) and with reference to the scheme proposed for *E. coli* transhydrogenase (*50*). The numbering system is based on the predictions of TM helices in the bovine enzyme (*16*). Gray circles with thickened lines show invariant residues; gray circles with thin lines show conserved residues (>11 identical out of 14 published sequences). Thanks to Gijs van Boxel for help with the figure.

step of transhydrogenase but to changes in conformation associated with nucleotide binding. However, the loci at which protonation/deprotonation reactions in the translocation pathway propagate the conformational changes, and the character of those conformational changes, are not yet understood. Two general cases can be considered. (a) Protons from the bacterial periplasm (or animal cell cytoplasm) proceed through dII and across dIII to the hydride-transfer site at the dI/dIII interface, where they effect the nucleotide-binding changes from close range. In this scenario, dII would have an essentially passive role delivering protons to the catalytic site at an electrochemical potential close to that of the periplasm. (b) The proton pathway involves only dII: a protein conformational change propagated within that component during the ion translocation steps is subsequently transmitted through dIII to the nucleotide-binding sites. In this model, a more substantial and longer range conformational change is envisaged, and this might be more consistent with the notion of site alternation that will be discussed below. Analyses of the available crystal structures argue against the first alternative in that they fail to reveal an H-bonded chain through dIII. Conceivably, the loops between TM helices, wrapping round dIII, could provide an insulated proton translocation pathway, but these loops are predicted to be quite short.

In the context of the second model, there are suggestions that βH91 and βN222 are not just passively involved in the proton translocation pathway. Mutations of these residues in the complete *E. coli* enzyme resulted in proteins with changed sensitivities to NADP(H)-dependent cleavage by trypsin of a site linking dII and dIII (*53*, *54*). It would seem that both residues are involved in the regulation of the properties of the NADP(H)-binding site by long-distance conformational changes. Other mutagenesis studies indicate the participation of amino acid residues linking dII to dIII (*E. coli*, βC260− βS266), and in the loop between TM helices 12 and 13 (*E. coli*, βD213), in this conformational change (*55*, *56*). However, observations of quite high levels of transhydrogenation and proton pumping in some of these mutants still await an explanation. Some have argued that effects of pH on the rates of reaction of some βH91 mutants can be explained in terms of a simple shift in the pK_a of the substituted protonatable group (*57*). Thus, the pH optimum for transhydrogenation was moved downward in the βH91E mutant, though more recent results show a similar downward shift in the pH optima of βH91K and βH91R (*58*). The interesting possibility that some of the mutations (e.g., βH91N) produce partially uncoupled or noncoupled proteins (*53*) requires further exploration. Note that βH91 is not invariant. In some organisms it is replaced by an asparagine, and though the substitution can be accompanied by the appearance of a new histidine on TM helix 3, this is not always the case.

The Binding Change Mechanism. Although the nature of the conformational changes involved in energy coupling in transhydrogenase has not yet been described, some properties of the intermediate states in the reaction can be recognized on the basis of kinetic and thermodynamic characteristics of the enzyme and its isolated components. A conceptual framework is provided by a "binding change" model (*4*, *6*, *8*, *59*); it contrasts with other conformationally coupled mechanisms outlined (*5*, *7*, *60*). The binding change model

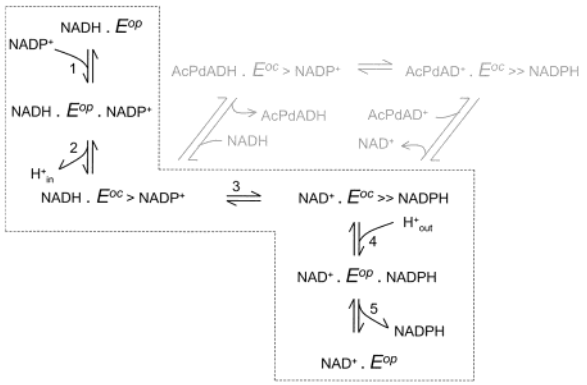

FIGURE 6: Binding change model for transhydrogenase and the cyclic transhydrogenation reaction (modified from refs *6*, *8*, and *59*). E^{op} and E^{oc} represent a dI:dII:dIII trimer of intact transhydrogenase with dIII in its open and occluded states, respectively. The binding change model (inside the dashed box). Following $NADP^+$ binding[a] (step 1), a proton is released[b] (step 2) to the inside aqueous phase to generate the occluded state. $NADP^+$ binds with moderate affinity (signified by ·) to the open state but is bound tightly (>) to the occluded state. Hydride transfer (step 3) takes place in the occluded state and proceeds to completion mainly because of the relative stabilization (≫) of the bound NADPH. Conversion back to the open state is then driven by protonation[b] from the outside aqueous phase (step 4). NADPH dissociates[a] from the open state (step 5). Note that the principles of the binding change mechanism form the basis for the alternating site model (see The Reciprocating, Alternating Sites of Transhydrogenase and Figure 7). [Footnotes: [a]The binding of NADH is shown to precede that of $NADP^+$, and the dissociation of NAD^+ is shown to follow that of NADPH. In fact, the nucleotides can bind at random to the open state (*72*). [b]An alternative situation, that protonation from the outside follows $NADP^+$ binding and that deprotonation to the inside precedes NADPH release, cannot be ruled out (*6*). Equivalent principles apply.] Cyclic transhydrogenation (step 3 together with the reactions outside the box) proceeds in an anticlockwise direction. It is a wholly artificial process: the reduction of $AcPdAD^+$ (an analogue of NAD^+) by NADH in the presence of $NADP^+$/NADPH. It was discovered with mitochondrial transhydrogenase (*73*) and explained (*74*, *75*), though the reaction was thought erroneously to be coupled to proton translocation. Experiments with detergent-dispersed *E. coli* enzyme led to a refined description (*59*). The cyclic reaction involves two hydride transfers (NADH → $NADP^+$ and NADPH → $AcPdAD^+$). It takes place either with $NADP^+$ and NADPH remaining bound to the enzyme (as shown) or $NADP^+$/NADPH can dissociate and then rebind. In dI_2dIII_1 complexes, the cyclic reaction is as fast as in the intact enzyme, but forward and reverse transhydrogenation are very slow since dIII is locked in the occluded state. As shown, the cyclic reaction is not associated with proton translocation.

has features in common with those proposed for the calcium-transporting ATPase and the F_1F_o ATP synthase, (see, e.g., refs *61* and *62*). The ease with which the chemical reaction of transhydrogenase can be measured in real time, and with which the protein can be resolved into its component parts and reconstituted, provides complementary experimental approaches to aid our understanding of the mechanisms of conformationally coupled ion translocators. Our mechanism is illustrated in Figure 6 (black symbols). It can be described by a set of "specificity rules", as defined (*63*):

(a) The dIII component of the dI:dII:dIII trimer can adopt an "open" state (or conformation) and an "occluded" state. The transfer of hydride ion equivalents between NAD(H) and NADP(H) can take place in the occluded state but not in the open state.

(b) $NADP^+$ and NADPH bound to the open state of dIII can readily exchange with nucleotides in the solvent. However, in the occluded state, this exchange is blocked.

(c) Interconversion between the two states during forward transhydrogenation is driven by inward proton translocation and is achieved by switching the proton access of a site in the protein from the bacterial periplasm to the cytoplasm (or from the animal cell cytoplasm to the mitochondrial matrix); the switch in solvent access is determined ("gated") by whether dIII is occupied by $NADP^+$ or by NADPH.

The specificity rules ensure that the enzyme is tightly coupled to the proton electrochemical gradient: the redox reaction is prevented from taking place without proton translocation and vice versa. The binding change model was proposed originally on the basis of experiments with the complete *E. coli* transhydrogenase (*59*). During "cyclic transhydrogenation" (Figure 6, gray symbols), $NADP^+$ and NADPH were found to bind with extremely high affinity at the hydride-transfer step, and yet the bound nucleotides were seen to exchange rapidly with those in the solvent during forward and reverse transhydrogenation, to allow turnover.

The isolated dI_2dIII_1 complex of *R. rubrum* transhydrogenase at neutral pH behaves as though its dIII is locked in the occluded state. Thus, it releases its bound $NADP^+$ (or NADPH) only extremely slowly (*23*, *64*), and it catalyzes very rapid hydride transfer between bound NADP(H) and NAD(H) (or their analogues) (*3*, *4*, *34*, *35*, *43*). Together, these factors result in the rapid, single-turnover burst kinetics of the redox reaction observed in stopped-flow experiments. As described above (see Detail at the Hydride-Transfer Site), the occluded character of the protein, and its propensity for rapid hydride transfer, can be readily understood from the available high-resolution structures: (a) bound $NADP^+$ is locked into its binding crevice by the loop E lid; (b) the NADP(H) nicotinamide ring, on the dIII ridge, can be brought into apposition with that of the NAD(H) in the dI cleft.

During the conversion of the occluded to the open state, the conformation of the loop E and helix D/loop D region must be loosened to allow rapid release of product NADPH and then rebinding of substrate $NADP^+$. We hypothesize that changes in the conformation of helix D/loop D, driven by proton translocation through dII, are the causal event for the opening of the site which will lead (a) to part of loop E peeling back from the surface of the dIII molecule and (b) to the movement of the NADP nicotinamide away from the NAD nicotinamide into a pocket which, in the crystal structure of isolated dIII, is occupied by a glycerol molecule (*38*). The amino acid triad, K164*-R165*-S166*, will presumably remain in place to maintain the specificity for NADP(H) over NAD(H) also in the open state. D132* in helix D/loop D might be important in the transition. In the high-resolution structures, it makes H-bonds with atoms in the nucleotide, with the backbone amide of A172* in loop E, and with a structural water molecule underneath this loop. It is inaccessible to the bulk solvent, and according to calculations using the MEAD program (*65*), its pK_a in the crystal structure is high, in the region of 9.8 (M. Jeeves, personal communication). During the opening of loop E and helix D/loop D, increased access to the solvent is expected to lower the pK_a of D132*. The negative charge resulting from the increased ionization might thus contribute to the

stabilization of the open state. Mutagenesis studies show that the equivalent of this residue in the *E. coli* enzyme is essential for transhydrogenation. Earlier proposals for the role of this residue included the suggestion that it forms part of the proton translocation pathway (*57*, *66*), but the X-ray structure of the dI_2dIII_1 complex indicates that D132* is some distance from the membrane-spanning region.

There are indications that, at low pH, isolated dIII adopts a conformation that more closely resembles the open state. Thus, in the low-pH form, the rate of NADP(H) release is increased more than 10-fold, and in complex with dI, the hydride-transfer reaction between bound nucleotides is blocked (*64*). It remains to be established whether protonation of isolated dIII at low pH is mechanistically related to the occluded → open interconversion that takes place in the complete transhydrogenase.

The directionality of proton translocation is achieved by switching access of the energy-transducing region of transhydrogenase (in dII or dIII) from the periplasm (protonation at high proton potential) to the cytoplasm (deprotonation at low proton potential). The switch is compulsorily linked with the open → occluded and occluded → open conformational changes, and its status is controlled by whether dIII is occupied by $NADP^+$ or NADPH. Chemical shift changes of backbone amide groups observed in HSQC NMR experiments on isolated dIII, when bound $NADP^+$ was substituted for NADPH (*36*, *41*), extend considerably from the nucleotide-binding site, but only in one direction: into the loop E lid and into the protruding helix D/loop D region (*38*, *39*). These changes indicate that either atomic displacements or charge redistribution (or both) accompanies the reduction of $NADP^+$. In view of the likely importance of loop E and helix D/loop D in nucleotide binding and interaction with dI and dII (see above), it was proposed that these rearrangements, in the complete protein, are a prerequisite for the proton switch (*38*).

The specificity rules define the coupling pathway, but for transhydrogenase to operate at an appreciable rate under physiological conditions, nucleotide-binding energies must be properly expressed: a general principle expounded in ref *63*. The dI and dIII components are located in an aqueous phase (the bacterial cytoplasm/mitochondrial matrix) in which the concentrations of the substrates NADH and $NADP^+$ are normally relatively low and those of the products NAD^+ and NADPH are normally relatively high. To turn over at a reasonable rate, we should expect the enzyme in the open state to bind NADH and $NADP^+$ with relatively high affinity (to promote substrate binding) and NAD^+ and NADPH with relatively low affinity (to promote product release). However, if this set of nucleotide-binding affinities were carried from the open state into the occluded state, then the K_{eq} of hydride transfer would be lowered (stabilization of reactants relative to products), leading to a restriction in the rate of turnover: it is immediately before and after the redox step that the rate-limiting protonation/deprotonation reactions associated with proton translocation drive interconversion of the open and occluded states (Figure 6). We proposed that, during the transition from the open to the occluded state, there is a change in the way the nucleotide-binding energy is expressed: the bound $NADP^+$ becomes destabilized relative to bound NADPH, thus increasing the on-enzyme equilibrium constant of hydride transfer (the $NADP^+$/NADPH redox potential is increased). Experimental support for an elevated on-enzyme equilibrium constant at this step in the occluded state (by >36-fold) was presented (*4*, *34*, *35*, *67*). Note that it is this change in binding affinities which *necessitates* the "occlusion" of the nucleotide: occlusion by loop E prevents the bound $NADP^+$ from being expelled from its binding site as it becomes destabilized relative to NADPH. To put this another way, the binding energies for different parts of the nucleotides are differentially expressed in the open and occluded states. The overall large increase in the expression of the nucleotide-binding energy in the occluded state, due to the increased interactions of the ribose and pyrophosphate groups with loop E, is accompanied by a relatively small decrease in the binding energy of the (oxidized) nicotinamide ring relative to that of the (reduced) dihydronicotinamide ring.

In Figure 6, the specificity rules are defined in terms of the interaction of NADP(H), but not of NAD(H), with the protein. We suggested that the binding properties of NADH and NAD^+ are not directly linked to the proton-binding and -release reactions of proton translocation: the NADH serves simply as a donor of hydride equivalents (*6*, *59*). Consistent with this, the rates of binding and release of NAD^+ and NADH are fast relative to turnover (*34*, *35*, *43*), and the K_d of isolated dI for NADH is only very weakly dependent on pH (*33*). However, there might be changes in NAD(H) binding during catalysis (*20*, *31*, *35*). Our current view (*35*) is that, during turnover of the complete enzyme, NADH binds predominantly to the dI associated with open dIII (K_d for NADH ~30 μM). As this dIII (with bound $NADP^+$) is converted to the occluded state, the associated dI−NADH site is shifted to a high K_d form (~300 μM), but NADH does not significantly dissociate during the short period of (fast) hydride transfer (*34*) and the reaction proceeds almost to completion (see above). The different conformations of NAD^+ seen in the asymmetric unit of the crystal structure of isolated dI (*32*) probably reflect these events in the complete enzyme. NAD(H) binding changes are not directly coupled to proton translocation [and in isolated dI_2dIII_1 complexes, NADH binding has to proceed through the "wrong" protein conformation (*35*)] but are advantageous (a) to keep the nicotinamide rings apart to prevent hydride transfer in the open state and (b) to permit relative stabilization of NAD^+ during hydride transfer in the occluded state.

The Reciprocating, Alternating Sites of Transhydrogenase. The complex formed from isolated dI and dIII is a stable dI_2dIII_1 heterotrimer in both the crystalline (*20*) and solution states (*31*). NMR experiments provide evidence for the existence of a dI_2dIII_2 tetramer, though the species has a very large dissociation constant (*36*). This is reflected in the fact that attempts to model a second dIII into the cleft of the dI(B) polypeptide of the heterotrimer, using the crystal coordinates, are prevented by side chain clashing of residues in helices αA, αB, and αF (*20*). Now, it is reemphasized that the dI_2dIII_1 complex catalyzes very rapid (single-turnover) rates of hydride transfer at its single dI/dIII interface and that the complete, intact transhydrogenase is effectively a dimer of dI:dII:dIII trimers. It is concluded that, during turnover of the complete enzyme, the nucleotide-binding sites at the two dI/dIII interfaces are *alternately* brought together to allow hydride transfer. The conformational changes responsible for the alternation must relate to

those involved in the nucleotide-binding changes that couple transhydrogenation to proton translocation. We proposed (*20*) that, as dI(A)/dIII(A) enters the open state to permit product release and substrate binding, dI(B)/dIII(B) enters the occluded state to permit hydride transfer: the A components and the B components run 180° out of phase (Figure 7A).

An analogy can be drawn with the F_1F_o ATP synthase. Also, in that enzyme, proton translocation through the membrane-spanning component, F_o, generates a conformational change (a continuous rotation) which is transmitted into the membrane peripheral component, F_1, where it results in the sequential binding changes at the three catalytic sites that effect ATP synthesis (*62*). In transhydrogenase, there are two, rather than three, catalytic sites, and the conformational changes cannot involve a continuous rotation; rather, proton translocation through this enzyme must drive *reciprocating* movements between rigid elements (TM helices in dII?) that are coupled to the open ↔ occluded transitions in dI/dIII. The out-of-phase synchronization of events in the A half and the B half of the protein can then be readily understood if equivalent helices (or clusters of helices) in dII(A) and dII(B) move against one another during proton binding/proton release. Movement of the motor helix (or helices) of dII(A) in one direction will generate the open state of dIII(A), and simultaneous movement of the equivalent helix (or helices) of dII(B) in the other direction will generate the occluded state of dIII(B). There is no information as to the nature of these movements: reciprocating rotations and translations can both be envisaged.

Experiments from Hatefi's laboratory have provided previous indications of the functional importance of the dimeric organization of bovine transhydrogenase (*68*, *69*). The enzyme is inhibited by dicyclohexylcarbodiimide (DCCD) and by fluorosulfonyl-*p*-benzoyladenosine (FSBA). Using radiolabeled compounds, it was shown that 100% inhibition was achieved when 0.5 mol of either DCCD or FSBA was bound per mole of transhydrogenase. It was proposed that only the "active protomer" is capable of rapid inhibitor binding. In terms of the alternating site mechanism, we suggest that the binding of DCCD/FSBA to one protomer is effective in blocking the turnover of both because they operate together as a single functional unit. Later experiments established that, at concentrations of nucleotide in the range 2−80 μM, one NADPH and one NADH bind to one dimeric molecule of bovine transhydrogenase. Again, this was taken as evidence of half-of-the-sites reactivity (*70*), and we would now interpret this in terms of the nucleotides binding only to one protomer.

It is appropriate to reconsider the βH91 and βN222 mutants (discussed in Coupling of Proton Translocation to Transhydrogenation) in the context of the alternating site mechanism. Recently, it was suggested that mutants of the complete *E. coli* transhydrogenase, in which either βH91 or βN222 is substituted with positively charged residues, appear to have their dIII components locked in the occluded state (*58*), and this is an interesting idea. However, we suggest that probably all transhydrogenases with mutations at βH91 of βN222 are compromised by an inability to alternate between the open and occluded states, so that *just one-half of the molecule* (i.e., one dI:dII:dIII trimer) is locked in the occluded conformation, while the other is locked in the open conformation. This is consistent with the observation that

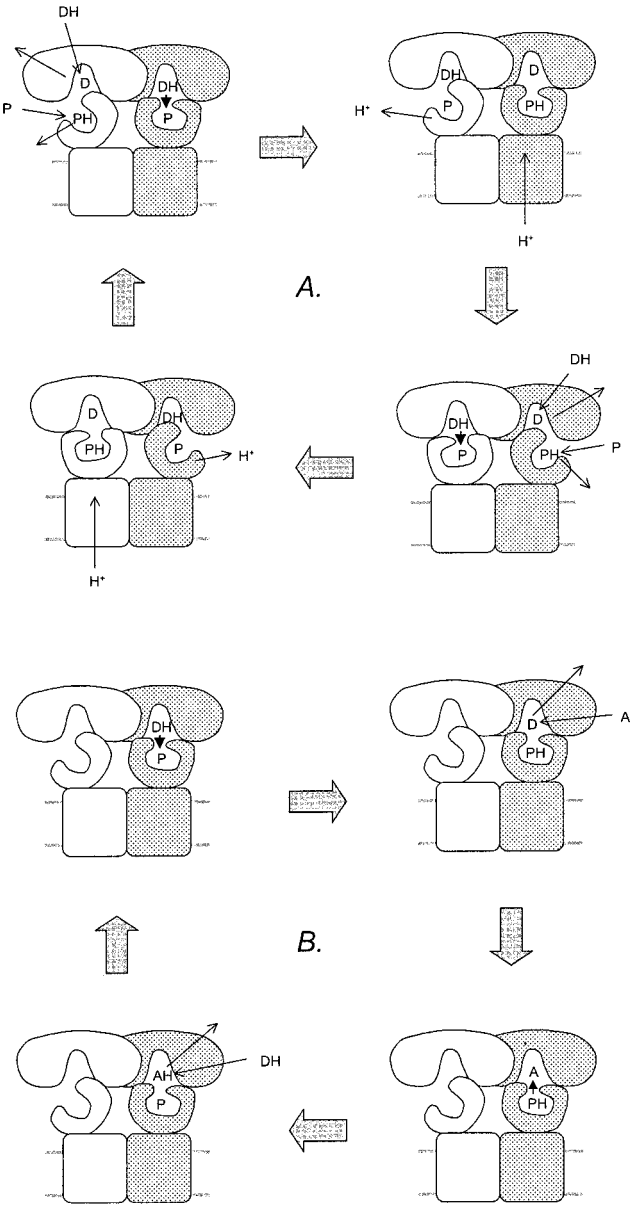

FIGURE 7: Transhydrogenase is a functional dimer. (A) The alternating site mechanism for forward transhydrogenation. D is NAD^+, DH is NADH, P is $NADP^+$, and PH is NADPH. At the top left, the white dI:dII:dIII trimer is in the open state and the gray trimer is in the occluded state. (B) A new perspective on cyclic transhydrogenation. A is $AcPdAD^+$, and AH is AcPdADH. Cyclic transhydrogenation takes place without alternation of the sites. Multiple turnovers can take place in the occluded state without any involvement of the open conformation. Thus, the reaction will proceed for a number (possibly a large number) of times only at the dI/dIII interface whose dIII is occluded. If protonation/deprotonation in the proton channel of dII does lead to conversion of this dIII into the open state, the cyclic reaction at this location will stop. However, simultaneous conversion of the dIII in the alternate dI/dIII interface from the open to the occluded state will initiate the cyclic reaction now at this site, provided that an $NADP^+$ or an NADPH is bound. Note that the binding of NADH and $AcPdAD^+$ during cyclic transhydrogenation is to a dI whose dIII is in the occluded state, whereas NADH binding during forward transhydrogenation is to a dI whose dIII is in the open state. In light of recent findings (*31*, *35*) (see The Binding Change Mechanism) we should now recognize that the affinity for NADH in the former condition is probably much lower than that in the latter. Taken together with the observed competition between NADH and $AcPdAD^+$ for the dI binding site (*76*), this explains why the cyclic reaction (*23*) is slower than that of its two hydride-transfer steps (*35*, *43*).

only up to about 0.8 mol of NADP(H)/mol of $\alpha_2\beta_2$ tetramer is found in the washed membranes (*58*). Forward and reverse transhydrogenation is inhibited in the mutants (see ref *9*) because interconversion of the open and occluded states is required for turnover. Cyclic transhydrogenation can proceed at low pH because, as explained (*6*), the reaction takes place within the occluded state (Figures 6 and 7). Most of the βH91 and βN222 mutants have a lag at the onset of cyclic transhydrogenation resulting from the slow binding of NADP(H) (*58*). We suggest that the lag represents the slow filling of the NADP(H) site in the occluded dI:dII:dIII trimer (where the cyclic reaction will proceed).

Final Comments: How Structural Elements Seen in the Crystal Structures of the dI_2dIII_1 Might Participate in the Alternating Site Mechanism. To further our understanding of how proton translocation drives the changes in nucleotide binding alternately in the two dI:dII:dIII trimers of transhydrogenase, more high-resolution structures of isolated components and complexes in different intermediate states and particularly of the complete enzyme are required. However, as indicated in this review, an examination of the first structures of dI, dIII, and dI_2dIII_1 already provides some indications of movements and changes in interaction (protein−protein and protein−nucleotide) that might occur during turnover. Our expectation is that the helix D/loop D region of dIII is pivotal in the energy transduction pathway. Bound NADP(H) in isolated dIII and in dI_2dIII_1 complexes is tightly occluded. In the complete enzyme, the shift between the occluded and open states, brought about by proton translocation through dII, will result from conformational changes in helix D/loop D and the consequent lowering/lifting of the adjacent loop E lid. In dI_2dIII_1 complexes, the only contact between dIII and dI.1(B) is via a few highly conserved residues in helix D/loop D (on dIII) and in the RQD loop (on dI.1). In contrast, there are extensive areas of contact between dIII and the core formed from dI.2(A) and dI.2(B). Thus, the changes in helix D/loop D that accompany the interconversion of the open and occluded states will be communicated to dI by moving the RQD loop, and therefore dI.1, against the relatively rigid dI.2 core, widening or narrowing the cleft.

The first steps in the binding of NADH to dI occur independently of the proton translocation-dependent binding changes in $NADP^+$. These steps involve the well-documented alterations in the conformation of the mobile loop, presumably with participation from the adjacent TAGP loop. When the bound $NADP^+$ has been occluded within dIII, and this has led to a reset in the conformation of dI (e.g., through interactions between helix D/loop D and the RQD loop), then the NADH can be prepared for hydride donation: its nicotinamide ring must be rotated (see Visualizing the Hydride-Transfer Step between Nucleotides Bound to dI and dIII in the dI_2dIII_1 Complex) into apposition with that of the $NADP^+$, and water must be expelled from the site. This will involve further conformational rearrangements of the polypeptide loops lining the site with changes in the width of the cleft. Conserved charged residues in the site (R127 and D135 in dI, R90* in dIII) are close enough to participate in the polarization of the nicotinamide rings to bias the (rapid) hydride-transfer reaction in favor of products; movements of the conserved aromatic residues (particularly Y235 in dI and Y171* in dIII) will be involved in these rearrangements to expel water and promote polarization. Complementary stepwise processes will be required to allow release of NAD^+ and the coupling of NADPH release to the completion of proton translocation.

In the context of our hypothesis, out-of-phase alternations at the two hydride-transfer sites are driven by the reciprocating primary events in dII. However, there is an indication that conformational changes across the dI dimer might coregulate events in the two cleft regions. Figure 3 illustrates the organization of the two helices, α6 and α11, that link the dI.1 and dI.2 domains in each of the dI protomers. Note that α6 has the RQD loop (involved in positioning the nicotinamide rings of NADH and $NADP^+$ in the hydride-transfer site) at its N-terminus and the β-hairpin (which forms a "wall" of the hydride-transfer site in the *partner* dI) at its C-terminus. The N- and C-termini of helix α11, on the other hand, are anchored in more central (and probably more rigid) regions in dI.1 and dI.2. The α6 and α11 helices from *partner* dI polypeptides are joined C-terminus to N-terminus, respectively, at an angle of about 30°, by hydrogen bonds at the point in α6 where the chain drops away to form the β-hairpin and in α11 where the helix breaks and the chain changes direction. The pair of abutting, double helices run alongside one another for about 62 Å with extensive hydrogen bond and van der Waals interactions between them. A network of mutual interactions between the two clefts is evident in this structure. Thus, events in the cleft of one dI polypeptide would result in conformational changes *across* the dimer interface to determine events in the other cleft and participate in the out-of-phase alternation. Rearrangements in the RQD loop of the dI(B) polypeptide (driven by changes in helix D/loop D of its bound dIII) can effect changes in the dI(A) cleft (a) by displacement of α6(B) to move β-hairpin(B) at the back of the dI(A) cleft and (b) by displacement of β-hairpin(A) and transmission along α6(A) to the RQD loop of dI(A). The α11 helices will be moved in tandem, resulting in rigid-body movement of dI.1 relative to dI.2, so that cleft A opens as cleft B closes.

During the past decade, the application of techniques in molecular biology, X-ray crystallography, and analysis by optical and NMR spectroscopy have led to significant advances in our understanding of proton-translocating transhydrogenase, but there is still much to be discovered about this fascinating protein. Some properties of transhydrogenase might be similar to those of other conformationally coupled ion pumps, and fundamental principles will probably continue to emerge. However, the evidence to date suggests that the conformational motions involved in coupling transhydrogenation to proton translocation will be unique. Our challenge is to establish the character of these processes and to discover how they effect the changes in nucleotide binding at the hydride-transfer site.

ACKNOWLEDGMENT

We thank Nick Cotton, Chris Weston, Dan Rodrigues, Gijs van Boxel, Owen Mather, Sarah Peake, and Mark Jeeves for discussion.

REFERENCES

1. Bizouarn, T., Sazanov, L. A., Aubourg, S., and Jackson, J. B. (1996) *Biochim. Biophys. Acta 1273*, 4−12.

2. Lee, C. P., Simard-Duquesne, N., Ernster, L., and Hoberman, H. D. (1965) *Biochim. Biophys. Acta 105*, 397−409.
3. Venning, J. D., Grimley, R. L., Bizouarn, T., Cotton, N. P. J., and Jackson, J. B. (1997) *J. Biol. Chem. 272*, 27535−27538.
4. Venning, J. D., and Jackson, J. B. (1999) *Biochem. J. 341*, 329−337.
5. Hatefi, Y., and Yamaguchi, M. (1996) *FASEB J. 10*, 444−452.
6. Jackson, J. B., Quirk, P. G., Cotton, N. P. J., Venning, J. D., Gupta, S., Bizouarn, T., Peake, S. J., and Thomas, C. M. (1998) *Biochim. Biophys. Acta 1365*, 79−86.
7. Rydstrom, J., Hu, X., Fjellstrom, O., Meuller, J., Zhang, J., Johansson, K., and Bizouarn, T. (1998) *Biochim. Biophys. Acta 1365*, 10−16.
8. Jackson, J. B., Peake, S. J., and White, S. A. (1999) *FEBS Lett. 464*, 1−8.
9. Bizouarn, T., Fjellstrom, O., Meuller, J., Axelsson, M., Bergkvist, A., Johansson, C., Karlsson, G., and Rydstrom, J. (2000) *Biochim. Biophys. Acta 1457*, 211−218.
10. Ambartsoumian, G., Dari, R., Lin, R. T., and Newman, E. B. (1994) *Microbiology 140*, 1737−1744.
11. Hickman, J. W., Barber, R. D., Skaar, E. P., and Donohue, T. J. (2001) *J. Bacteriol.* (in press).
12. Rydstrom, J., and Hoek, J. B. (1988) *Biochem. J. 254*, 1−10.
13. Sazanov, L. A., and Jackson, J. B. (1994) *FEBS Lett. 344*, 109−116.
14. Mercer, N. A., McKelvey, J. R., and Fioravanti, C. F. (1999) *Exp. Parasitol. 91*, 52−58.
15. Clark, C. G., and Roger, A. J. (1995) *Proc. Natl. Acad. Sci. U.S.A. 92*, 6518−6521.
16. Yamaguchi, M., Hatefi, Y., Trach, K., and Hoch, J. A. (1988) *J. Biol. Chem. 263*, 2761−2767.
17. Clarke, D. M., Loo, T. W., Gillam, S., and Bragg, P. D. (1986) *Eur. J. Biochem. 158*, 647−653.
18. Williams, R., Cotton, N. P. J., Thomas, C. M., and Jackson, J. B. (1994) *Microbiology 140*, 1595−1604.
19. Yamaguchi, M., and Hatefi, Y. (1994) *J. Bioenerg. Biomembr. 26*, 435−445.
20. Cotton, N. P. J., White, S. A., Peake, S. J., McSweeney, S., and Jackson, J. B. (2001) *Structure 9*, 165−176.
21. Diggle, C., Hutton, M., Jones, G. R., Thomas, C. M., and Jackson, J. B. (1995) *Eur. J. Biochem. 228*, 719−726.
22. Yamaguchi, M., and Hatefi, Y. (1995) *J. Biol. Chem. 270*, 28165−28168.
23. Diggle, C., Bizouarn, T., Cotton, N. P. J., and Jackson, J. B. (1996) *Eur. J. Biochem. 241*, 162−170.
24. Yamaguchi, M., and Hatefi, Y. (1997) *Biochim. Biophys. Acta 1318*, 225−234.
25. Fjellstrom, O., Johansson, C., and Rydstrom, J. (1997) *Biochemistry 36*, 11331−11341.
26. Fjellstrom, O., Bizouarn, T., Zhang, J., Rydstrom, J., Venning, J. D., and Jackson, J. B. (1999) *Biochemistry 38*, 415−422.
27. Peake, S. J., Venning, J. D., and Jackson, J. B. (1999) *Biochim. Biophys. Acta 1411*, 159−169.
28. Weston, C. J., White, S. A., and Jackson, J. B. (2001) *FEBS Lett. 488*, 51−54.
29. Diggle, C., Cotton, N. P. J., Grimley, R. L., Quirk, P. G., Thomas, C. M., and Jackson, J. B. (1995) *Eur. J. Biochem. 232*, 315−326.
30. Yamaguchi, M., Wakabayashi, S., and Hatefi, Y. (1990) *Biochemistry 29*, 4136−4143.
31. Venning, J. D., Rodrigues, D. J., Weston, C. J., Cotton, N. P. J., Quirk, P. G., Errington, N., Finet, S., White, S. A., and Jackson, J. B. (2001) *J. Biol. Chem. 276*, 30678−30685.
32. Buckley, P. A., Jackson, J. B., Schneider, T., White, S. A., Rice, D. W., and Baker, P. J. (2000) *Structure 8*, 809−815.
33. Bizouarn, T., Diggle, C., and Jackson, J. B. (1996) *Eur. J. Biochem. 239*, 737−741.
34. Venning, J. D., Peake, S. J., Quirk, P. G., and Jackson, J. B. (2000) *J. Biol. Chem. 275*, 19490−19497.
35. Pinheiro, T. J. T., Venning, J. D., and Jackson, J. B. (2001) *J. Biol. Chem.* (in press).
36. Quirk, P. G., Jeeves, M., Cotton, N. P. J., Smith, K. J., and Jackson, J. B. (1999) *FEBS Lett. 446*, 127−132.
37. Prasad, G. S., Sridhar, V., Yamaguchi, M., Hatefi, Y., and Stout, C. D. (1999) *Nat. Struct. Biol. 6*, 1126−1131.
38. White, S. A., Peake, S. J., McSweeney, S., Leonard, G., Cotton, N. N. J., and Jackson, J. B. (2000) *Structure 8*, 1−12.
39. Jeeves, M., Smith, K. J., Quirk, P. G., Cotton, N. P. J., and Jackson, J. B. (2000) *Biochim. Biophys. Acta 1459*, 248−257.
40. Bergkvist, A., Johansson, C., Johansson, T., Rydstrom, J., and Karlsson, B. G. (2000) *Biochemistry 39*, 12595−12605.
41. Johansson, C., Bergkvist, A., Fjellstrom, O., Rydstrom, J., and Karlsson, B. G. (1999) *FEBS Lett. 458*, 180−184.
42. Eventoff, W., and Rossmann, M. G. (1975) *CRC Crit. Rev. Biochem. 111*, 111−140.
43. Venning, J, D., Bizouarn, T., Cotton, N. P. J., Quirk, P. G., and Jackson, J. B. (1998) *Eur. J. Biochem. 257*, 202−209.
44. Fisher, R. R., and Guillory, R. J. (1971) *J. Biol. Chem. 246*, 4687−4693.
45. Wu, Y. D., and Houk, K. N. (1991) *J. Am. Chem. Soc. 113*, 2352−2358.
46. Bizouarn, T., Diggle, C., Quirk, P. G., Grimley, R. L., Cotton, N. P. J., Thomas, C. M., and Jackson, J. B. (1996) *J. Biol. Chem. 271*, 10103−10108.
47. Grimley, R. L., Quirk, P. G., Bizouarn, T., Thomas, C. M., and Jackson, J. B. (1997) *Biochemistry 36*, 14762−14770.
48. Quirk, P. G., Smith, K. J., Thomas, C. M., and Jackson, J. B. (1999) *Biochim. Biophys. Acta 1412*, 139−148.
49. Studley, W. K., Yamaguchi, M., Hatefi, Y., and Saier, M. H. (1999) *Microb. Comp. Genomics 4*, 173−186.
50. Meuller, J., and Rydstrom, J. (1999) *J. Biol. Chem. 274*, 19072−19080.
51. Bragg, P. D., and Hou, C. (2000) *Biochem. Biophys. Res. Commun. 273*, 955−959.
52. Bizouarn, T., Meuller, J., Axelsson, M., and Rydstrom, J. (2000) *Biochim. Biophys. Acta 1459*, 284−290.
53. Glavas, N. A., Hou, C., and Bragg, P. D. (1995) *Biochemistry 34*, 7694−7702.
54. Bragg, P. D., and Hou, C. (1999) *Arch. Biochem. Biophys. 363*, 182−190.
55. Althage, M., Bizouarn, T., and Rydstrom, J. (2001) *Biochemistry 40*, 9968−9976.
56. Yamaguchi, M., and Hatefi, Y. (1995) *J. Biol. Chem. 270*, 1−7.
57. Hu, X., Zhang, J. W., Fjellstrom, O., Bizouarn, T., and Rydstrom, J. (1999) *Biochemistry 38*, 1652−1658.
58. Bragg, P. D., and Hou, C. (2001) *Arch. Biochem. Biophys. 388*, 299−307.
59. Hutton, M. N., Day, J. M., Bizouarn, T., and Jackson, J. B. (1994) *Eur. J. Biochem. 219*, 1041−1051.
60. Hu, X., Zhang, J. W., Persson, B., and Rydstrom, J. (1995) *Biochim. Biophys. Acta 1229*, 64−72.
61. Lee, A. G., and East, J. M. (2001) *Biochem. J. 356*, 665−683.
62. Stock, D., Gibbons, C., Arechaga, I., Leslie, A. G., and Walker, J. E. (2000) *Curr. Opin. Struct. Biol. 10*, 672−679.
63. Jenks, W. P. (1983) *Curr. Top. Membr. Transp. 19*, 1−18.
64. Rodrigues, D. J., Venning, J. D., and Jackson, J. B. (2001) *Eur. J. Biochem. 268*, 1430−1438.
65. Bashford, D., and Gerwert, K. (1992) *J. Mol. Biol. 224*, 473−486.
66. Meuller, J., Hu, X., Buntoff, C., Olausson, T., and Rydstrom, J. (1996) *Biochim. Biophys. Acta 1273*, 191−194.
67. Peake, S. J., Venning, J. D., Cotton, N. P. J., and Jackson, J. B. (1999) *Biochim. Biophys. Acta 1413*, 81−91.
68. Phelps, D. C., and Hatefi, Y. (1984) *Biochemistry 23*, 4475−4480.
69. Phelps, D. C., and Hatefi, Y. (1985) *Biochemistry 24*, 3503−3507.
70. Yamaguchi, M., and Hatefi, Y. (1993) *J. Biol. Chem. 268*, 17871−17877.
71. Cserzo, M., Wallin, E., Simon, I., von Heijne, G., and Elofsson, A. (1997) *Protein Eng. 10*, 673−676.
72. Hanson, R. L. (1979) *J. Biol. Chem. 254*, 888−893.
73. Wu, L. N. Y., Earle, S. R., and Fisher, R. R. (1981) *J. Biol. Chem. 256*, 7401−7408.

74. Fisher, R. R., and Earle, S. R. (1982) in The Pyridine Nucleotide Coenzymes (Everse, J., Anderson, B. M., and You, K. S., Eds.) pp 279−324, Academic Press, New York.
75. Enander, K., and Rydstrom, J. (1982) *J. Biol. Chem. 257*, 14760−14766.
76. Bizouarn, T., Grimley, R. L., Cotton, N. P. J., Stilwell, S., Hutton, M., and Jackson, J. B. (1995) *Biochim. Biophys. Acta 1229*, 49−58.

BI012078D